Contents lists available at SciOpen

Food Science and Human Wellness

journal homepage: https://www.sciopen.com/journal/2097-0765

China Food Publishing Co.

Precision *N*-glycoproteomics reveals the essential role of the extracellular matrix in tropomyosin allergy in a mouse model

Guirong Liu[a], Qianwei Wang[a], Yibo Luo[b], Lijuan Sun[a], Ruolin Song[a], Huilian Che[a], Changqi Liu[c,*], Xiaohui Guo[a,*]

[a] *College of Food Science and Nutritional Engineering, China Agricultural University, Beijing 100083, China*
[b] *Department of Dermatology and Venereology, West China Hospital, Sichuan University, Sichuan 610000, China*
[c] *School of Exercise and Nutritional Sciences, College of Health and Human Services, San Diego State University, California 92182, USA*

ARTICLE INFO

Article history:
Received 7 February 2024
Received in revised form 27 March 2024
Accepted 7 April 2024

Keywords:
Seafood allergy
Tropomyosin
Extracellular matrix
Precision
N-Glycoproteomics
Intestinal barrier
Glycome

ABSTRACT

Approximately 2.5% of the global population experience allergic reactions to seafood, making it one of the most prevalent and life-threatening allergies. Seafood allergy can lead to the disruption of the intestinal barrier, possibly due to aberrant intestinal glycosylation. In this study, the mechanisms underlying seafood allergy were explored through the lens of intestinal glycobiology. Mice were sensitized with tropomyosin, resulting in significant increases in allergy symptom scores, specific antibody and T helper 2 cytokine levels. Intestinal damage was confirmed by histopathology, as well as by assessments and levels of diamine oxidase and claudin-1. Moreover, alterations in glycosylated proteins within the jejunum were analyzed using high-throughput mass spectrometry and the pGlyco3.0 search engine. Precision *N*-glycoproteomics analysis yielded 2 283 glycosylation peptides corresponding to 655 unique glycosylation sites on 399 proteins. Differential expression and enrichment analyses revealed that differentially expressed glycoproteins were significantly enriched in the extracellular matrix (ECM)-receptor interaction pathway and focal adhesion pathway. In conclusion, tropomyosin sensitization leads to intestinal glycome changes, accompanied by remodeling of the intestinal ECM. Our research establishes an essential theoretical basis for targeting the intestinal glycome and ECM remodeling in a precise and fine-tuned manner for the treatment of food allergies.

1. Introduction

Seafood allergy ranks among the most prevalent and severe allergies, affecting 2.5% of the global population[1]. In Asia, it accounts for up to 37.8% of reported food allergy reactions among older children and adults[2]. Unlike allergies caused by eggs and milk, shellfish allergies are typically lifelong disorders that significantly impair quality of life[3]. Moreover, there are limited options for preventing anaphylactic reactions in individuals with seafood allergy. Hence, the primary treatment is to avoid offending foods[2]. Considering the high frequency and severity of seafood allergy, there is an urgent need to determine its underlying mechanism for the development of innovative treatments.

Most patients with seafood allergy react to tropomyosin[4-5], a common shellfish allergen with high homology among various seafoods[6-7]. Lam et al.[8] found that tropomyosin sensitization could induce varying degrees of damage within the small intestine. The intestine serves as the first barrier against food allergens, and damage to the intestinal barrier and disruptions in intestinal flora are associated with food allergies[9-10]. Moreover, epithelial polysaccharides play a role in supporting intestinal mucosal homeostasis and

* Corresponding authors.
E-mail address: changqi.liu@sdsu.edu (C.Q. Liu); guoxiaohui@cau.edu.cn (X.H. Guo)
Peer review under responsibility of Beijing Academy of Food Sciences.

Publishing services by Tsinghua University Press

http://doi.org/10.26599/FSHW.2024.9250247

barrier integrity, and glycosylation disorders may disrupt intestinal homeostasis[10-11]. Zhang et al.[12] found that mutations in phosphoglutamate 3 (PGM 3) decreased intestinal *N*- and *O*-glycosylation, linking these changes to food allergies. Yao et al.[10] reported that sialylation of mucin-2 by ST6GALNAC1 (a sialyltransferase) can prevent the intestinal flora from breaking down mucin, thereby preserving mucus integrity and the intestinal barrier. However, rencent research has mostly focused on inflammatory bowel disease (IBD)[13-14], and the role of glycosylation in the disruption of the intestinal barrier caused by food allergies remains unclear. Therefore, elucidating the alterations in the intestinal glycome during allergic reactions is crucial for establishing a solid theoretical foundation for developing novel and effective treatments and for understanding of the pathogenesis of food allergies.

In this study, we employed high-throughput mass spectrometry acquisition combined with the pGlyco3.0 search engine to analyze changes in intestinal protein glycosylation in mice with tropomyosin allergy. Our findings lay the groundwork for exploring the regulatory role of glycosylation in food allergies.

2. Materials and methods

2.1 Extraction, purification, and identification of tropomyosin

Tropomyosin of brown shrimp was isolated and purified following the procedure described by Zhang et al.[15]. Specifically, raw shrimp muscles were minced and homogenized in 0.01 mol/L PBS buffer (pH 7.4; 4:1 (*V*/*m*)) using a homogenizer (Shanghai Specimen Model Factory, Shanghai, China). The homogenate was centrifuged at 10 000 × *g* for 15 min, and the resulting pellet was collected. This process of washing, homogenization, and centrifugation was repeated 3 times to effectively remove sarcoplasmic proteins. Subsequently, the final precipitate underwent 3 washes with cold absolute acetone (−20 ℃). The residues were placed on filter paper and dried overnight following the final wash. The dried powder was suspended in 8-fold (*m*/*V*) of Tris-HCl buffer (1 mol/L KCl, 0.5 mmol/L DTT, 20 mmol/L Tris-HCl, pH 7.5), and extraction was carried out with stirring at 4 ℃ overnight. The resulting solution was then centrifuged at 15 000 × *g* for 15 min. The supernatant, after passing through filter papers, underwent isoelectric precipitation at pH 4.5 adjusted with 1 mol/L HCl. This mixture was kept at 4 ℃ for 4 h and then centrifuged at 15 000 × *g* for 15 min. After dissolving the precipitate in PBS, it was subjected to isoelectric precipitation again at a pH of 4.5 using 1 mol/L HCl. The resulting isoelectric precipitate was dissolved in PBS and adjusted to pH 7.6 with 1 mol/L NaOH. It was then subjected to ammonium sulfate fractionation at 41% saturation, kept at 4 ℃ for 4 h, and centrifuged at 15 000 × *g* for 15 min. This process of ammoniumsulfate fractionation was repeated once. The resulting precipitate was dialyzed (10 kDa, Solarbio Inc., Beijing, China) in ultrapure water (UNIQUE Water Purification System, RO-DI® Technology Inc., Xiamen, China) at 4 ℃ for 48 h, followed by heating in a boiling water bath for 10 min. After thorough cooling in ice water, the boiled solution was centrifuged at 15 000 × *g* for 15 min. The supernatant containing purified TM was passed through filter papers, lyophilized using a vacuum freeze drier (Labconco Inc., Kansas, USA), and stored at −20 ℃.

Purity of tropomyosin was analyzed using reduced SDS-PAGE with 4%–20% polyacrylamide gels (8012011, Dakewe Inc., Beijing, China) and a Tris-Gly-SDS running buffer (50 mmol/L Tris, 40 mmol/L glycine, and 3 mmol/L SDS). Pre-stained protein standards with molecular weights of 10, 15, 25, 35, 40, 55, 70, 100, 130, and 180 kDa (BN27001; Biorigin Inc., Beijing, China) were used as references. The soluble protein content of the samples was determined using the BCA method (BN27109; Biorigin Inc.). Protein samples were boiled in reduced SDS sample buffer (BN27020; Biorigin Inc.) for 5 min and then loaded in equal amounts. Following electrophoresis, the gels were stained with a staining solution (0.1% Coomassie brilliant blue R250 (C8430; Solarbio Inc.), 10% acetic acid, and 45% methyl alcohol).

Biological identification of tropomyosin was performed using Q-Exactive Orbitrap Mass Spectrometry. The protein bands of tropomyosin were excised from the polyacrylamide gels and subjected to in-gel trypsin digestion, according to the protocol reported by De Angelis et al.[16]. The resulting peptide mixture was analyzed using a high-performance liquid chromatography (HPLC) system (Thermo Fisher Scientific Inc., Waltham, MA, USA) coupled to a Q-Exactive™ Plus Hybrid Quadrupole-Orbitrap™ mass spectrometer. Samples were loaded via an automatic sampler into a C_{18} trap column (300 μm × 5 mm, 5 μm, 100 Å) and then separated using an analytical C_{18} column (75 μm × 150 mm, 3 μm, 100 Å) with a flow rate of 300 nL/min. After processing the raw mass spectrometry spectra, proteins were identified by searching against the Decapoda database (https://www. uniprot.org/uniprotkb? query=Decapoda, accessed on 15 September 2023) obtained from UniProtKB using the MASCOT software. The database-searching parameters were as follows: enzyme: trypsin; max missed cleavages: 1; peptide mass tolerance: ± 20 × 10^{-6}; fragment mass tolerance: 0.6 Da; peptide confidence: high; the filtration parameter was as follows: peptide FDR ≤ 0.05.

Allergenicity assessment of tropomyosin was performed using serological test. The collection and use of serum have been reviewed and approved by the Human Research Ethics Committee of China Agricultural University (CAU-HR2021015). Sera from 6 Chinese shrimp allergic patients with a documented history of shrimp anaphylaxis and 2 non-allergic volunteers were used to evaluate the immunoglobulin E (IgE) binding ability of the isolated tropomyosin. Information of the allergic patients and volunteersis provided in Table 1. Blood samples were clotted for 2 h at 25 ℃ and then centrifuged at 825 × *g* for 15 min at 4 ℃ to obtain serum. The serum samples were stored at − 80 ℃ before analyses. The blood collection process was approved by the patients. IgE dot-blot assays were carried out by applying the tropomyosin solution (2 μg protein/spot) to nitrocellulose membranes (0.22 μm; Biosharp, Hefei, China; 2 duplicates per membrane), blocking for 1 h at 25 ℃ in TBS-T plus 5% non-fat dry milk with shaking, and then incubating with the serum diluted at 1:10 overnight at 4 ℃[17]. The membrane was washed with TBS-T 6 times. Immune complexes were detected using horseradish peroxidase (HRP)-conjugated goat anti-human IgE antibody (ab73901; Abcam Inc., Cambridge, UK) and enhanced chemiluminescence (ECL) plus reagent (34580; Thermo Fisher Scientific Inc.).

2.2 Animals and experimental protocol

2.2.1 Experimental animals

Five-week-old female specific pathogen-free C57BL/6N mice were purchased from Vital River Laboratories (SYXK (Jing) 2020-0052; Beijing, China) and housed at (23 ± 3) ℃ and 40%–70% relative humidity with a 12-h light/dark cycle. Mice had free access to

Table 1
Subject information.

Number	Gender	Age	Allergen
1	Male	31	Dust mites, mulberry, cat dandruff, milk, shrimp, beef, shellfish, crab, cashew, pineapple, green branches
2	Male	18	Cockroach, amaranth, chicken egg white, milk, shrimp, shellfish, crab, mango, cashew, pineapple, green branch
3	Female	9	Cockroach, amaranth, chicken egg white, milk, shrimp, shellfish, crab, mango, cashew, pineapple, green branch
4	Female	32	Dust mites, house dust, mulberry, dog dandruff, cockroach, amaranth, chicken protein, shrimp, mango, cashew, pineapple, dwarf ragweed, walnut sycamore poplar
5	Female	24	Dust mites, mulberry, cat fur dander, dog fur dander, cockroach, chicken egg whites, milk, shrimp, beef, crab
6	Female	10	Dust mites, house dust, mulberry, cat dandruff, cockroach, amaranth, chicken protein, shrimp, crab, mango, cashew, pineapple
7	Female	24	No history of specific allergies
8	Female	45	No history of specific allergies

distilled water and a shrimp-protein-free diet and were adaptively fed for 7 days before the experiment. The animal study was reviewed and approved by the China Agricultural University's Experimental Animal Ethics Committee (No.7 AW70101202-4-1).

2.2.2 *Sensitization of mice to tropomyosin*

A total of 12 mice were randomly assigned to the control and allergy groups using stratified randomization based on their body weight ($n = 6$ per group). On days 0, 7, 14, and 21, mice in the allergy group received intraperitoneal injections of 100 μg tropomyosin (dissolved in 100 μL PBS) with 100 μL aluminum adjuvant (77161; Thermo Fisher Scientific Inc.). Mice in the control group were given equivalent PBS and aluminum adjuvant without tropomyosin. On days 28 and 35, both groups were challenged with tropomyosin (1 mg/mL) *via* gavage (Fig. 1).

2.3 *Clinical symptoms and body temperature*

Following the challenge on day 28, the mice were observed for 60 min. The clinical symptoms of each mouse were scored according to Li et al.[18]. The following scoring system was used: 0, no symptoms; 1, scratching and rubbing around the nose and head; 2, puffiness around the eyes and mouth, diarrhea, pilar erecti, reduced activity with or without an increased respiratory rate; 3, wheezing, labored respiration, and cyanosis around the mouth and tail; 4, no activity after prodding or tremor and convulsion; 5, death. The internal anorectal temperature was measured within 60 min to evaluate the body temperature change on day 35.

2.4 *Determination of specific antibody levels in serum*

The levels of mouse serum tropomyosin-specific IgE and IgG1 were determined by indirect enzyme-linked immunosorbent assay (ELISA) according to Sepulveda et al.[19]. Briefly, 100 μL of tropomyosin solution (10 μg/mL) was added to each well of a 96-well plate. The plate was left overnight at 4 °C and washed 3 times with 350 μL of PBST solution per well. Next, the plate was blocked using a 0.01 g/mL BSA (V900933; Sigma-Aldrich, Burlington, USA) solution and incubated at 37 °C for 2.5 h. After washing, 50 μL of serum (diluted 5-fold for sIgE detection and 5 000-fold for IgG1) were added to each well and incubated at 37 °C for 2 h. Following 6 washes with PBST solution, HRP-conjugated rat anti-mouse IgE (MA5-16781; Abcam Inc.) or goat anti-mouse IgG1 (18-4015-82; Abcam Inc.) secondary antibodies were added and incubated for 1 h at 37 °C. After another round of 6 washes with PBST solution, 100 μL of TMB substrate solution (P0209; Beyotime Inc., Shanghai, China) was added to each well. The plate was incubated at 37 °C for 15 min, and the reaction was stopped by 2 mol/L H_2SO_4. The absorbance at 450 nm was measured by a Varioskan Flash Spectral Scanning Multimode Reader (Thermo Fisher Scientific Inc.).

2.5 *Determination of inflammatory mediator levels in serum*

On day 35, mice were anesthetized (60 min after the challenge) using isoflurane and subsequently euthanized by cervical dislocation to produce blood and organ samples. Blood was collected from the mice at the eye socket vein. The collected blood was subjected to

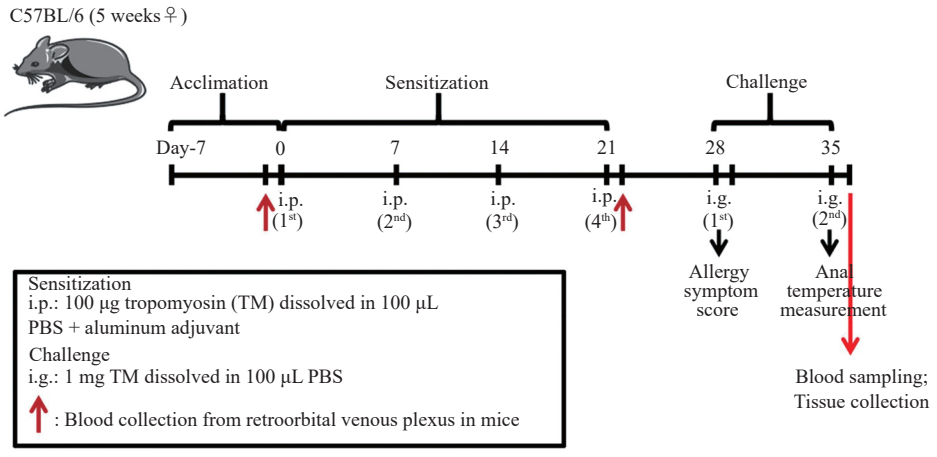

Fig. 1 Experimental flow chart of tropomyosin-sensitized mice.

centrifugation at 4 ℃ and 825 × *g* for 15 min. The serum was obtained and stored at –80 ℃ . The levels of interleukin (IL)-4 (DG30082M), IL-13 (DG30030M), interferon (IFN)-γ (DG30056M), histamine (DG30046M), and diamine oxidase (DAO) (DG30229M) were determined using ELISA kits (Dogesce, Beijing, China).

2.6 Histopathological analysis

The spleen, duodenum, jejunum, ileum, and colon were harvested for histopathological examinations. Staining and pathological analyses were performed asdescribed in our previous paper[20]. Tissue slices were observed under a light microscope (Leica Microsystems, Wetzlar, Germany).

2.7 Real-time quantitative PCR

Total RNA was extracted from spleen samples using TRIzol™ Reagent (15596026: Thermo Fisher Scientific Inc.) according to the protocol established by Donald et al.[21]. Subsequently, the RNA (1 μg) was used to synthesize cDNA using the HiScript III 1st Strand cDNA Synthesis Kit (Vazyme Inc., Nanjing, China). The mRNA expression levels of *Il-4*, *Il-6*, *Il-10*, *Il-13*, *Ifng*, and *Actb* were measured using an ABI 7500 Fast Real-Time PCR device (Life Technologies, Carlsbad, CA, USA) along with Taq Pro Universal SYBR qPCR Master Mix (Vazyme Inc.). Specific primer sequences are shown in Table 2. Relative mRNA levels were analyzed using the $2^{-\Delta\Delta CT}$ method[22].

2.8 Western blotting

Proteins were isolated from the duodenum, jejunum, ileum and colon (50–70 mg) using RIPA buffer supplemented with a protease inhibitor PMSF (P0013K; BioriginInc.), and their concentration was determined using the BCA protein assay kit (BN27109; Biorigin Inc.). These proteins were subsequently separated by SDS-PAGE as described in section 2.1. Afterward, the proteins were transferred onto polyvinylidene fluoride (PVDF) membranes (IPVH00005; Millipore, Darmstadt, Germany). Subsequently, the electroblotted membranes were incubated with anti-claudin 1 pAb (Ab32246; Lianke Bio Inc., Hangzhou, China). Immune complexes were detected using HRP-conjugated anti-rabbit IgG (BN20601; Biorigin Inc.) and ECL plus reagent (34580; Thermo Fisher Scientific Inc.)

2.9 Precision N-glycoproteomic analysis

2.9.1 Protein digestion

The jejunum of 2 randomly selected mice from each group was combined into a single sample, and 3 samples from each group were prepared for precision *N*-glycoproteomics analysis. The samples from the allergic and control groups were designated as tropomyosin (TM) treated model group and assessment datum (AD) group, respectively. After determining the protein concentration, using the BCA protein assay (BN27109; Biorigin Inc.), 1 mg of protein per condition was transferred to an Eppendorf tube and adjusted to 200 μL with 8 mol/L urea. First, 20 μL of 0.5 mol/L TCEP was added and incubated at 37 ℃ for 1 h. Next, 40 μL of 1 mol/L iodoacetamide was added and incubated for 40 min at room temperature, protected from light. Next, 5 volumes of −20 ℃ pre-chilled acetone were added to precipitate proteins overnight. After 2 washes with 1 mL of pre-chilled 90% acetone aqueous solution, the precipitates were re-dissolved in 100 mmol/L TEAB. Proteins were digested overnight at 37 ℃ using sequence-grade modified trypsin (Promega, Madison, WI, USA) at a 1:50 ratio (enzyme:protein, *m*/*m*). The peptide mixture was desalted with the C18 ZipTip, measured using the Pierce™ quantitative colorimetric peptide assay (23275), and lyophilized using a SpeedVac.

2.9.2 Enrichment of glycopeptides

The lyophilized peptides were re-dissolved in 80% acetonitrile (ACN) and 1% trifluoroacetic acid (TFA) and loaded onto a ZIC-HILIC micro-column with 30 mg of ZIC-HILIC particles (Millipore) on a C8 disc. After passing the flow through the column 4 more times, the column was washed with 80% ACN and 1% TFA. Glycopeptides were eluted with 0.1% TFA, 25 mmol/L NH_4HCO_3, and 50% ACN and dried by vacuum centrifugation.

2.9.3 Nano-HPLC-MS/MS analysis

The peptides were re-dissolved in 10 μL solvent A (0.1% formic acid in H_2O) and analyzed by nanospray LC-MS/MS using an Orbitrap Fusion Lumos Tribrid (Thermo Fisher Scientific Inc.) coupled to an EASY-nano-LC 1200 system (Thermo Fisher Scientific Inc.) without the trap column. A 3 μL peptide sample was loaded onto a C_{18} spray tip column (15 cm × 75 μm i.d., Acclaim PepMap; Thermo Fisher Scientific Inc.) and separated at a flow rate of 300 nL/min over a 180-min gradient elution from 3% to 32% solution B (0.1% formic acid in ACN). An electron spray voltage of 2 kV was used.

The mass spectrometer was run under data-dependent acquisition mode, automatically switching between MS and MS/MS mode. The specific parameters were as follows: (1) MS: scan range (*m*/*z*) was 350–2 000; resolution was 120 000; automatic gain control (AGC) target was 500 000; maximum injection time was 50 ms; included charge state was 2–6; dynamic exclusion after *n* times, *n* = 1; dynamic exclusion duration 15 s; each selected precursor was subject to 1

Table 2
Primer sequences of RT-qPCR

Gene	Primer sequences (forward)	Primer sequences (reverse)
Il-13	CCTGGCTCTTGCTTGCCTT	GGTCTTGTGTGATGTTGCTCA
Il-4	TGTGGTGTTCTTCGTTGCTGTGAG	TACCAGGAGCCATATCCACGG ATG
Ifng	ATGAACGCTACACACTGCATC	CCATCCTTTTGCCAGTTCCTC
Il-10	GCTCTTACTGACTGGCATGAG	CGCAGCTCTAGGAGCATGTG
Il-6	TAGTCCTTCCTACCCCAATTTCC	TTGGTCCTTAGCCACTCCTTC
Actb	AAGTGTGACGTTGACATCCGTAAAG	CAGCTCAGTAACAGTCCGCCTAGA

higher-energy C (dissociative) collision dissociation (HCD)-MS/MS; HCD-MS/MS: isolation window was 4; detector type was Orbitrap; resolution was 15 000; AGC target was 500 000; maximum injection time was 250 ms; collision energy was 30%; stepped collision mode on, energy difference of ± 10% (10% as the absolute value in the Orbitrap Fusion).

2.9.4 Data analysis

Tandem mass spectra were processed using pGlyco 3.0 (pFind Studio). The searches were performed against the protein database UniProt-mouse (ver. 2022, 21992 entries) and the pGlyco glycan database (species: mouse), assuming the digestion enzyme trypsin. pGlyco 3.0 was searched with a fragment ion mass tolerance of 2×10^{-5} and a parent ion tolerance of 1×10^{-5}. Carbamidomethylation (C) was specified as a fixed modification. Oxidation (M) was specified as a variable modification. The filtering criterion for glycopeptides was set at 1% total FDR. For the quantitative analysis of site-specific glycosylation, pGlyQuant (pFind Studio) was used for label-free quantification.

2.10 Statistical analysis

All experiments were performed in triplicate and data are representative of three independent parallel tests. All results are expressed as the mean ± standard deviation (SD). Statistical analyses were performed using GraphPad Prism 9.0.0 (GraphPad Software, Insightful Science Inc., San Diego, CA, USA), and comparisons between groups were conducted using *t*-tests. $P < 0.05$ was considered significant.

3. Results

3.1 Tropomyosin sensitization induces a typical IgE-mediated T helper 2 (Th2)-type immune response in mice

Tropomyosin was extracted and purified following the methods described by Zhang et al.[23]. The isolated protein appeared as a single band with a molecular weight of 35–48 kDa, as determined by SDS-PAGE (Fig. 2A, lanes 8 and 9). Subsequent analyses by QE mass spectrometry and a comparison against the MASCOT database further

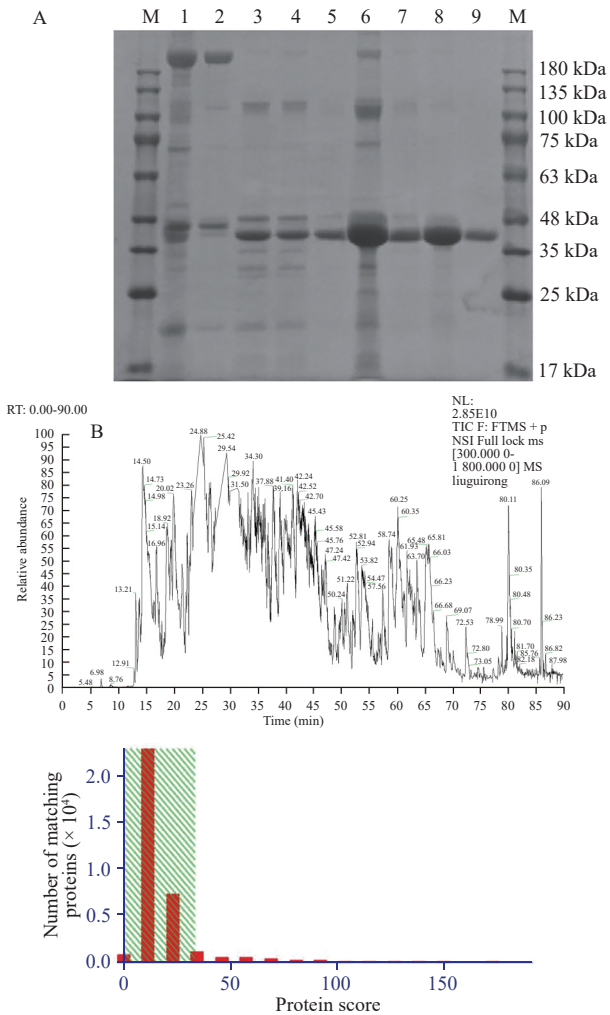

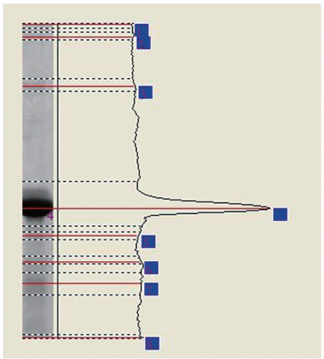

Protein sequence coverage: 94%

Matched peptides shown in red.

1 MDAIKKKMQA MKLEKDNAMD RADTLEQQNK EANNRAEKSE EEVHNLQKRM
51 QQLENDLDQV QESLLKANIQ LVEKDKALSN AEGEVAALNR RIQLLEEDLE
101 RSEERLNTAT TKLAEASQAA DESERMRKVL ENRSLSDEER MDALENQLKE
151 ARFLAEEADR KYDEVARKLA MVEADLERAE ERAETGESKI VELEEELRVV
201 GNNLKSLEVS EEKANQREEA YKEQIKTLTN KLKAAEARAE FAERSVQKLQ
251 KEVDRLEDEL VNEKEKYKSI TDELDQTFSE LSGY

Match serial number	Molecular weight	Matching score	Biochemical identity
GenBank: EU410 072.1	32 830	70 695	Lit v 1 (*Litopenaeus vannamei*)

Fig. 2 Extraction, purification, and identification of shrimp tropomyosin. (A) Changes in protein components during the extraction of tropomyosin from brown shrimp analyzed by SDS-PAGE. The purity of tropomyosin was analyzed using ImageJ; Lane 1, shrimp myofibrillar proteins; Lane 2, protein fractions from acetone extract; Lane 3, extracted protein fractions; Lane 4, protein fractions after secondary isoelectric point precipitation; Lane 5, protein fractions after secondary ammonium sulphate precipitation; Lane 6, protein fractions before dialysis; Lane 7, protein fractions after dialysis; Lane 8, protein fractions after removal of heat-sensitive proteins; Lane 9, purified tropomyosin after freeze-drying; and M-protein standards. (B) Biological identification of tropomyosin by QE mass spectrometry; (C) Immunoreactivity of tropomyosin by serological testing (dot-blot, 2 duplicates per membrane)).

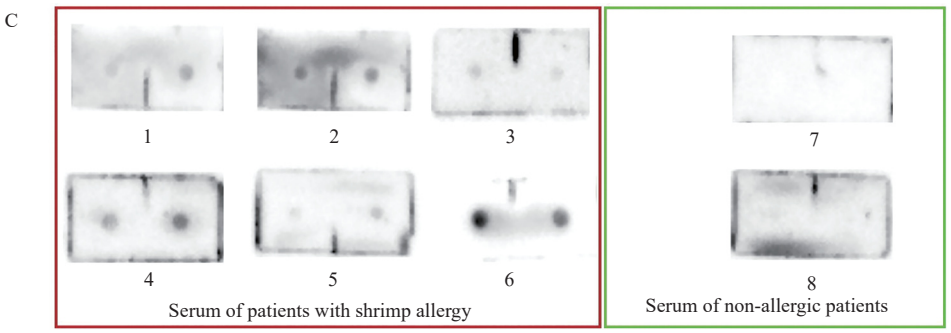

Fig. 2 (*Continued*)

confirmed that the extracted protein was tropomyosin (Fig. 2B). Moreover, the allergenicity of the isolated tropomyosin was verified by a serological test (Table 1 and Fig. 2C), indicating its readiness for sensitization.

Mice were sensitized to tropomyosin, as described in section 2.2[24] (Fig. 1). Following 10-fold high-dose stimulation on days 28 and 35, mice in the allergic group exhibited a substantial decrease in body temperature (Fig. 3A) and an increase in allergic symptom scores (Fig. 3B). The serum levels of tropomyosin-specific IgE and IgG_1 in allergic mice were significantly higher than those in the control group (Figs. 3C and D), indicating the occurrence of both rapid and delayed food anaphylaxis[25-26]. Moreover, since food allergies are typical Th2 immune responses, characterized by IgE binding to the Fcε receptors on effector cells such as mast cells and basophils, the activation of these cells leads to the release of histamine and other preformed mediators[27]. Therefore, serum levels of the typical Th2 cytokines IL-4, IL-13, Th1 cytokine IFN-γ, and histamine were examined. As shown in Figs. 3E-H, mice in the allergy group exhibited considerably higher levels of IL-4, IL-13, and histamine than those of mice in the control group, while the IFN-γ level did not differ significantly between the groups. Furthermore, inflammatory symptoms in the spleen, including vascular loosening, endothelial swelling, and shedding, were observed, along with higher transcription levels of allergy-related cytokines (*Il-6*, *Il-10*, and *Il-4*) (Figs. 3I and J). These results indicated that mice were successfully sensitized to tropomyosin.

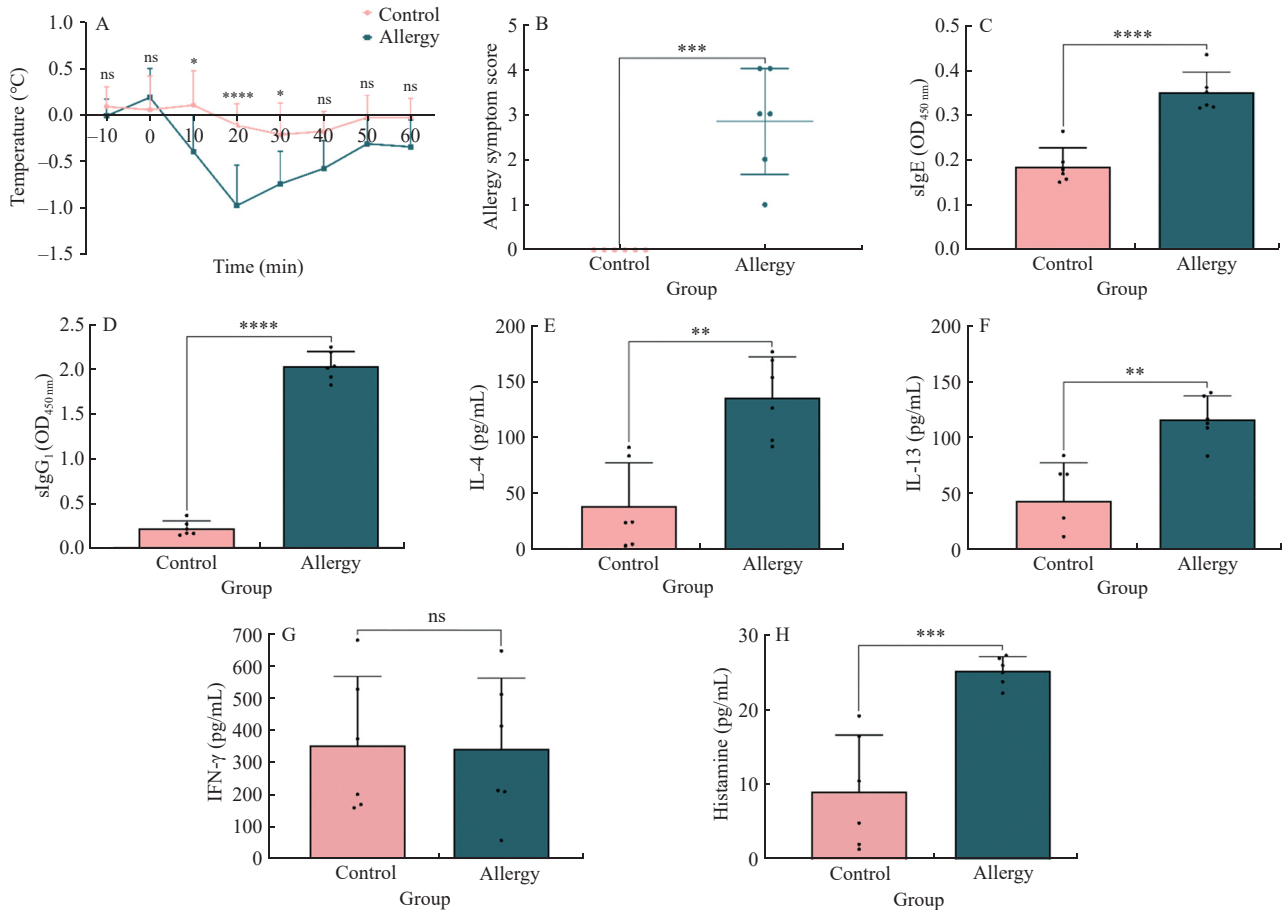

Fig. 3 Changes in allergic indexes in mice sensitized with tropomyosin. (A) Body temperature; (B) allergic clinical score; (C) sIgE; (D) sIgG1; (E) IL-4; (F) IL-13; (G) IFN-γ; (H) histamine; (I) Hematoxylin and Eosin staining of the spleen; (J) qPCR analysis of the transcript levels of allergy-related inflammatory factors in the spleen. ns, no significance; $*P < 0.05$, $**P < 0.01$, $***P < 0.001$, $****P < 0.000\ 1$.

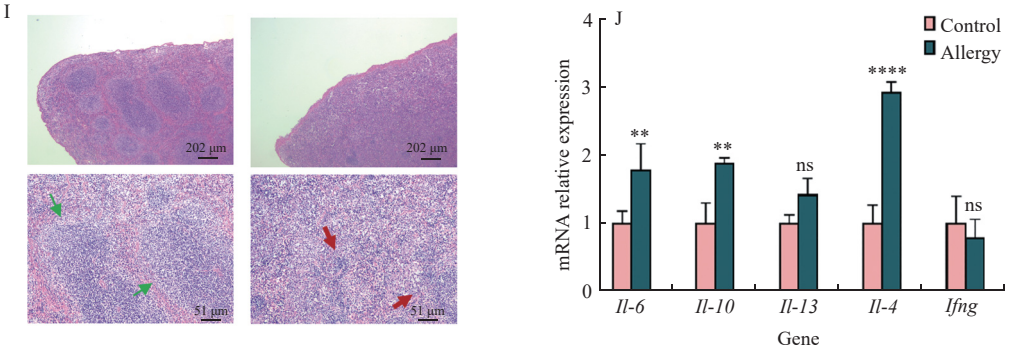

Fig. 3 (*Continued*)

3.2 Tropomyosin sensitization causes varying degrees of intestinal damage in mice

Tropomyosin sensitization can cause damage to the intestinal barrier in the small intestine[8], while epithelial polysaccharides support intestinal barrier integrity[10,28]. To better understand how intestinal glycosylation regulates food allergies, we examined the integrity of the intestinal barrier. As shown in Fig. 4A, the intestinal villus structure in the control group remained intact, displaying no obvious inflammatory symptoms. However, mice in the allergy group exhibited varying degrees of damage in the duodenum, jejunum, ileum, and colon, including the shortening and shedding of intestinal villi. Notably, the extent of damage decreased from the small intestine to the large intestine, consistent with the findings of Lam et al.[8]. In line with the histopathological analysis, the expression level of the tight junction protein claudin-1 in the small intestine was significantly lower in the allergy group than in the control group (Fig. 4B). Moreover, levels of serum DAO, an indicator of intestinal barrier breakdown[29], were significantly higher in the allergy group than in the control group (Fig. 4C).

In summary, tropomyosin sensitization induced intestinal damage, particularly in the small intestine in mice. Consequently, the severely injured jejunal tissue was utilized for further examination of alterations in intestinal protein glycosylation.

3.3 Mouse jejunal tissue is rich in N-glycosylation modifications

A precision *N*-glycoproteomics analysis was employed to examine changes in intestinal protein glycosylation induced by tropomyosin sensitization[30]. The depth exhibited minimal variation among samples, demonstrating strong reproducibility, stability, and reliability (Fig. 5A, 10 replicates). A total of 2 283 glycosylated peptides corresponding to 655 unique glycosylation sites on 399 proteins were identified (Fig. 5B). Comparison with UniProt *N*-glycan site information (https://www.uniprot.org/) was performed to validate the modified sites and identify new modified sites. Among the *N*-glycosylation sites identified in this study, 452 were validated in UniProt, and 203 were unique (Fig. 5C).

Qualitative analyses of glycosylated peptides, filtered at a total FDR of 1% for quality control, revealed *N*-glycosylation heterogeneity at both micro- and macro-levels. Most glycosylation sites exhibited two or more alterations, contributing to glycosylation micro-heterogeneity (Fig. 5D). Additionally, 33.8% of glycoproteins had more than 1 glycosylation sites, and 11.2% had 5 or more glycosylation sites, indicating high glycosylation heterogeneity (Fig. 5E). Notably, these proteins were mainly associated with cell adhesion and migration (LAMC1, LAMA5, ITA1, ITA6, CAD17, MUC2, and LRP1), endocytosis, antigen processing (LY75), the apoptotic process (HYOU1), and metabolism (ACE, AMPN, CUBN, A0A571BF69, F8VPT3, and F8VQM5).

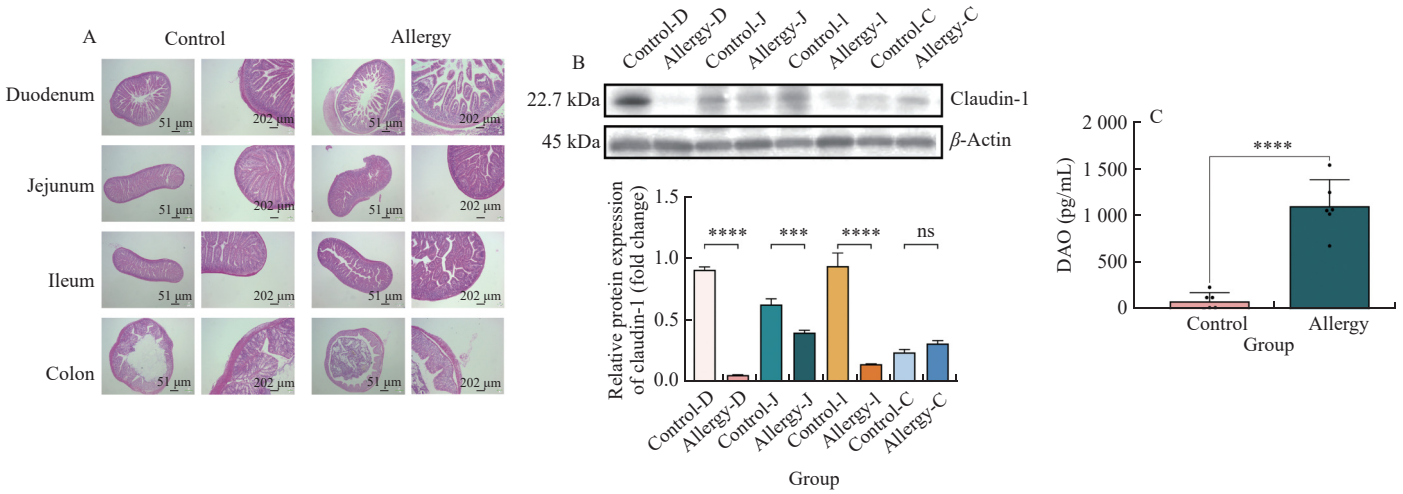

Fig. 4 Evaluation of the integrity of the intestinal barrier in mice with tropomyosin allergy. (A) Hematoxylin and Eosin staining of the intestine; (B) Western blotting and semi-quantitative analysis of the expression level of the intestinal tight junction protein caludin-1, evaluated using ImageJ, (D, duodenum; J, jejunum; I, ileum; C, colon); (C) diamine oxidase (DAO) level. ns, no significance; **** $P < 0.000\ 1$.

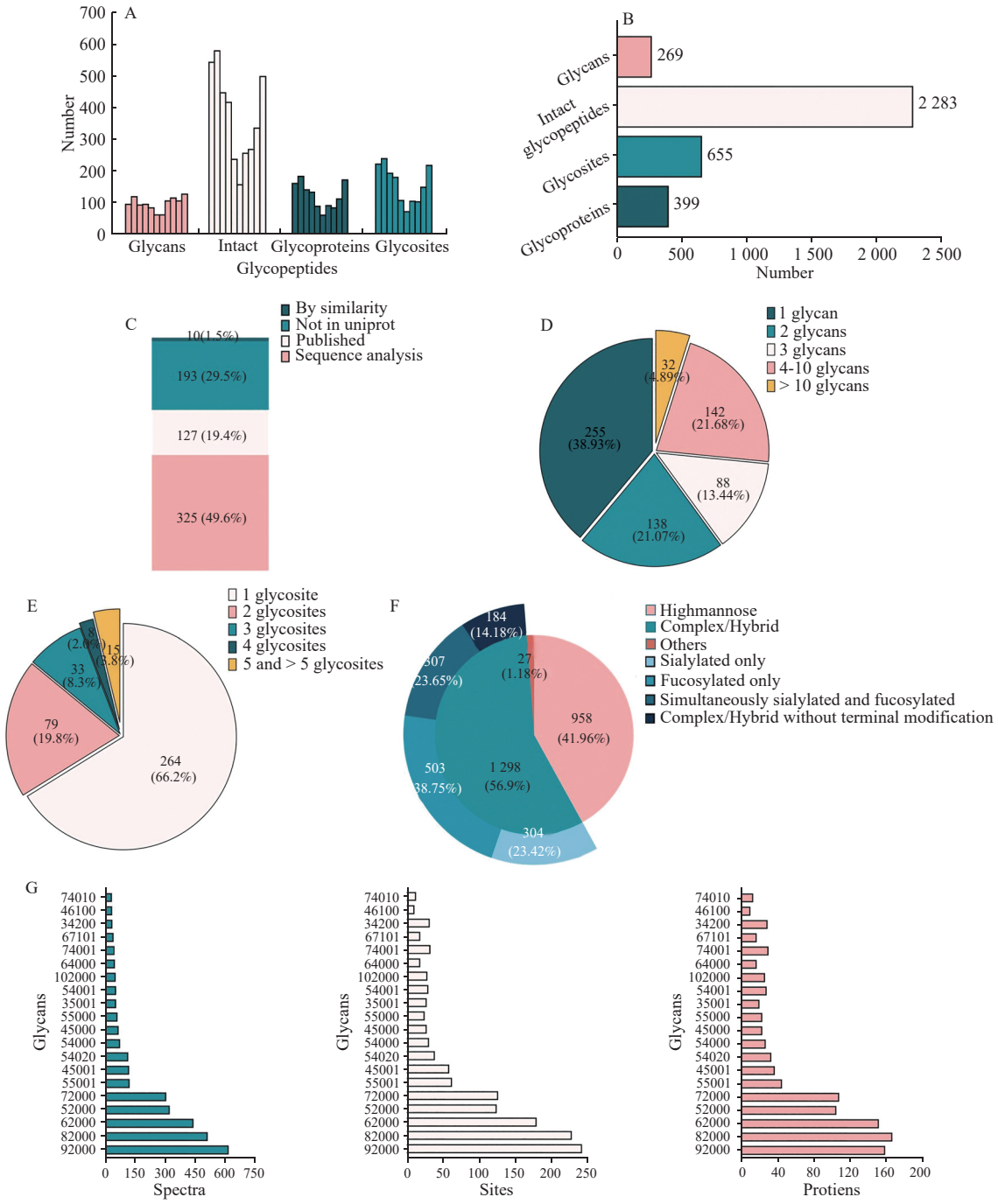

Fig. 5 Qualitative and quantitative study of sugar types in an intestinal glycoprotein precision *N*-glycoproteomic analysis of mice with tropomyosin allergy. (A) Intra-assay repeatability statistical analysis; (B) quantitative results of precision *N*-glycoproteomics identification; (C) comparative analysis of *N*-glycosylation sites of glycopeptides in the UniProt database (note: "not in Uniprot" indicates glycosylation sites that do not appear in the database); (D) pie chart of them sugar type distribution corresponding to a single glycosylation site; (E) pie chart of the glycosylation modification site distribution corresponding to a single protein. (F) Pie chart of the *N*-glycosylation type distribution; (G) qualitative analysis of the sugar type of the Top 20 sugar chain.

The types of glycosylation in the gut were examined according to the classification criteria outlined in Table 3. As shown in Fig. 5F, the numbers of high-mannose and complex/hybrid modified glycopeptides were similar (958 *vs*. 1 298), with 85.82% of complex/hybrid modified glycopeptides ending with sialylation or fucosylation. The number of spectra, glycoproteins, and glycosylation sites for the 20 most frequently detected sugar chains are shown in Fig. 5G. The distribution of modification types was comparable to the overall glycosylation modification type distribution.

Table 3
Basis for the identification of *N*-glycosylation types.

N-Glycosylation type	Sugar composition
High mannose	N = 2, A = 0, F = 0, pH = 0
Complex/hybrid	N > 2
Sialylation	A > 0
Fucosylation	F > 0
Glycan-phosphorylation (MP6)	pH > 0

Note: N, GlcNAc; A, NeuAc or NeuGc; F, Fuc; H, Hex; pH, phosphateHex.

3.4 Distinct N-glycosylation profiles for jejunal proteins in allergic mice

Fig. 6A illustrates the repeatability of the samples through a principal component analysis (PCA). TM-1 in the allergic group exhibited substantial dispersion, possibly attributed to the lower sensitivity of an individual animal, as evidenced in Fig. 3 (e.g., 1 mouse displayed low allergy symptom scores and serum IL-4 and IL-13 levels). Consequently, both 6-sample (Fig. 6A) and 4-sample (Fig. 6B) analyses were conducted. Based on the analyses of sample dispersion along both PC1 and PC2, TM-1 and AD-3 were excluded from the 4-sample analysis.

Differentially expressed proteins in the control and allergy groups were identified using screening criteria of fold change > 1.2 or < 0.83 and $P < 0.05$ (t-test). The analysis of 6 samples yielded 64 differently expressed glycoproteins, including 24 down-regulated (green) and 40 up-regulated proteins (pink) (Fig. 6C and Table S1). Differentially expressed glycoproteins

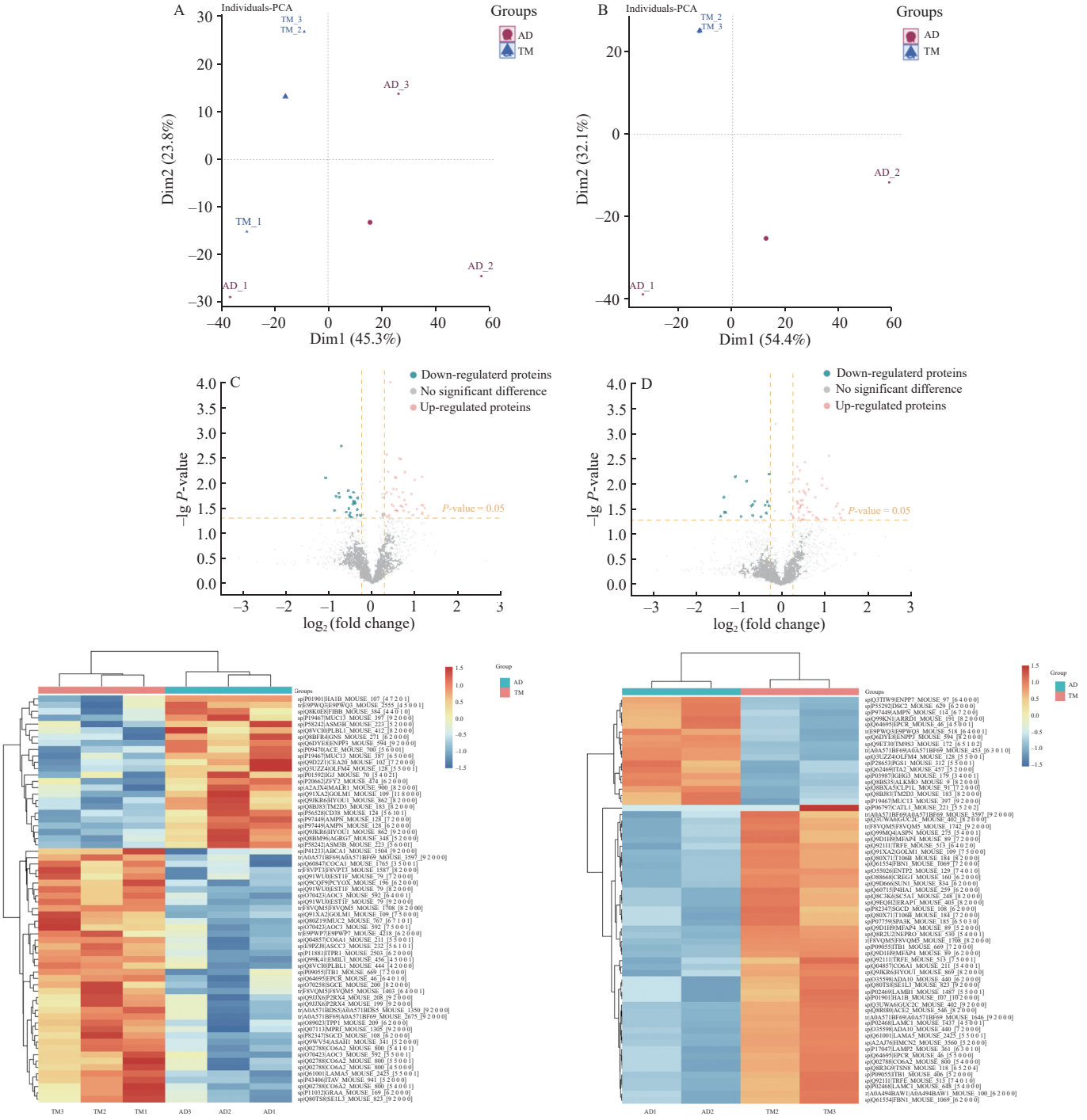

Fig. 6 Quantitative analysis of precision *N*-glycoproteomics of differentially expressed glycoproteins in the intestines of mice with tropomyosin allergy. Principal component analysis (PCA) results for (A) 6 or (B) 4 samples. Volcano plot illustrating differentially expressed glycoproteins in the allergicmouse intestine compared with the control group for (C) 6 or (D) 4 samples. Heatmap depicting the fold changes in the expression of the allergic mouse intestine compared with expression in the control group as determined by precision *N*-glycoproteomic analysis, (E) 6-samples analysis; (F) 4-samples analysis).

from 4 samples included 17 down-regulated (green) and 46 up-regulated (pink) proteins (Fig. 6D and Table S2). To further understand group similarity and variation, a hierarchical clustering analysis (HCA) of the differentially expressed proteins was performed (Figs. 6E and F). HCA results highlighted discernible variation in intestinal glycosylated proteins between the control and tropomyosin allergy groups, offering insights into potential markers linked to allergic responses. Congruence in differentially expressed glycoproteins was observed between the 6-sample and 4-sample analyses, demonstrating the reliability of the analytical methodologies in detecting significant differences in glycoprotein expression levels between the studied groups, despite slight variation in sample sizes and methodological constraints.

3.5 Tropomyosin sensitization drives intestinal extracellular matrix remodeling

To investigate the role of intestinal glycosylation regulation in tropomyosin allergy, differentially expressed proteins between the control and allergic groups were evaluated by additional functional enrichment analyses. Gene Ontology (GO) enrichment analysis revealed significant enrichment in cellular components, including extracellular region part, extracellular space, protein complex involved in cell adhesion, collagen trimer, and membrane part. Moreover, the differentially expressed proteins were enriched in biological processes, such as cell-substrate adhesion, cell adhesion mediated by integrin, and heterotypic cell-cell adhesion (Fig. 7, Tables S3 and S4).

In agreement with the findings of the GO analysis, Kyoto Encyclopedia of Genes and Genomes (KEGG) enrichment analysis identified the ECM-receptor interaction and focal adhesion pathway as the most enriched pathways (Figs. 8A and B, Table S5). Moreover, enrichment for the PI3K-Akt signaling pathway, known to be upregulated in food allergies[31], was also detected. The upregulation of the PI3K-Akt signaling pathway has been linked to intestinal tight junction damage induced by TNF-α[32], supporting the decrease in tight junction protein levels and increase in intestinal permeability in the allergy group in our study. Up-regulated glycoproteins were also involved in pathways related to absorption and metabolism, such as the protein digestion and absorption pathway, carbohydrate digestion and absorption pathway (in both 4- and 6-sample analyses), galactose metabolism pathway, lysosome pathway, purine metabolism pathway

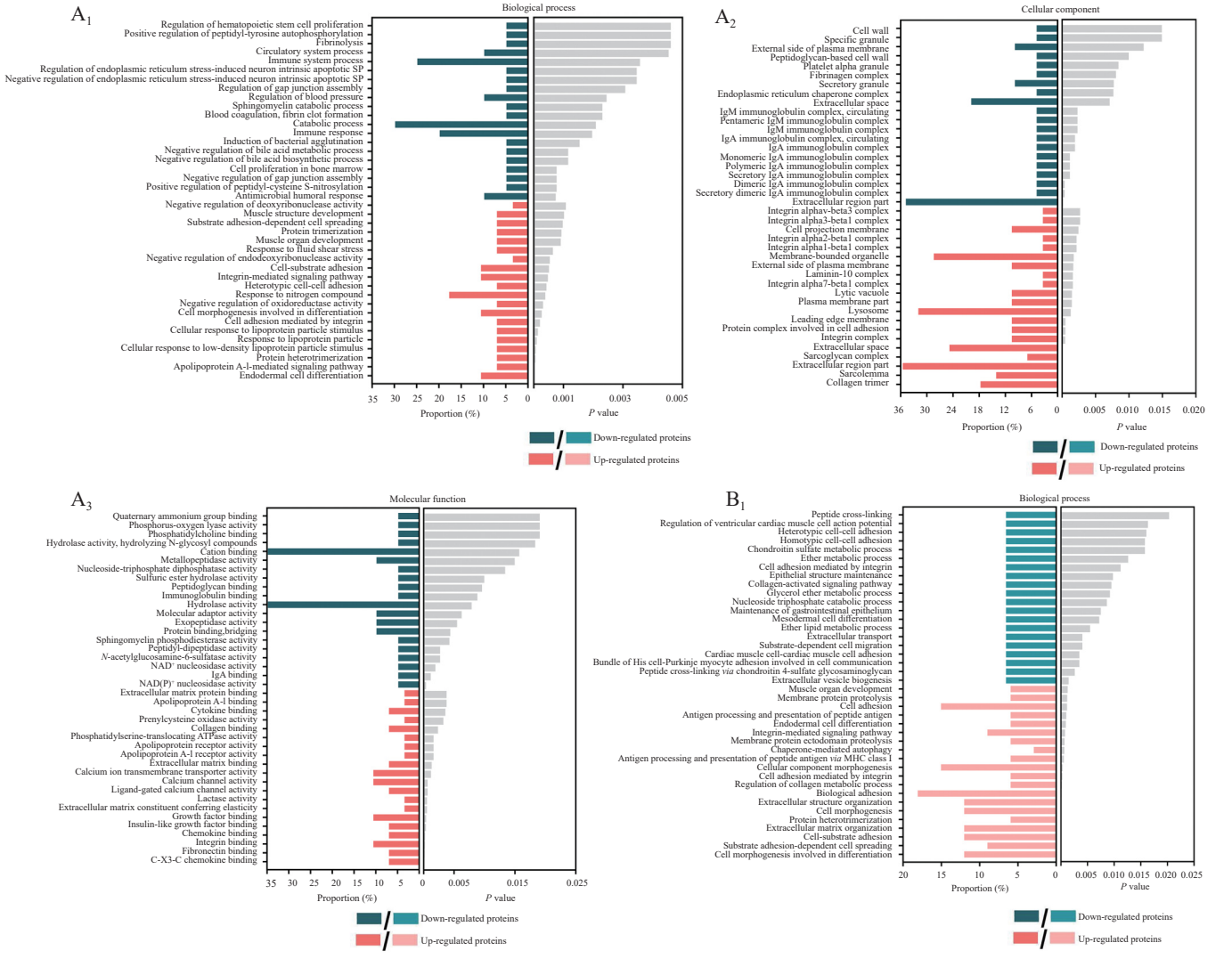

Fig. 7 GO enrichment analysis of differentially expressed glycoproteins in the intestine of mice with tropomyosin allergy identified by precision *N*-glycoproteomics. (A) Six-samples analysis; (B) four-samples analysis. In panel (B_3), oxidoreductase activity (paired donors/monooxygenase) denotes oxidoreductase activity, acting on paired donors, with incorporation or reduction of molecular oxygen, incorporation of one atom of oxygen (into the other donor).

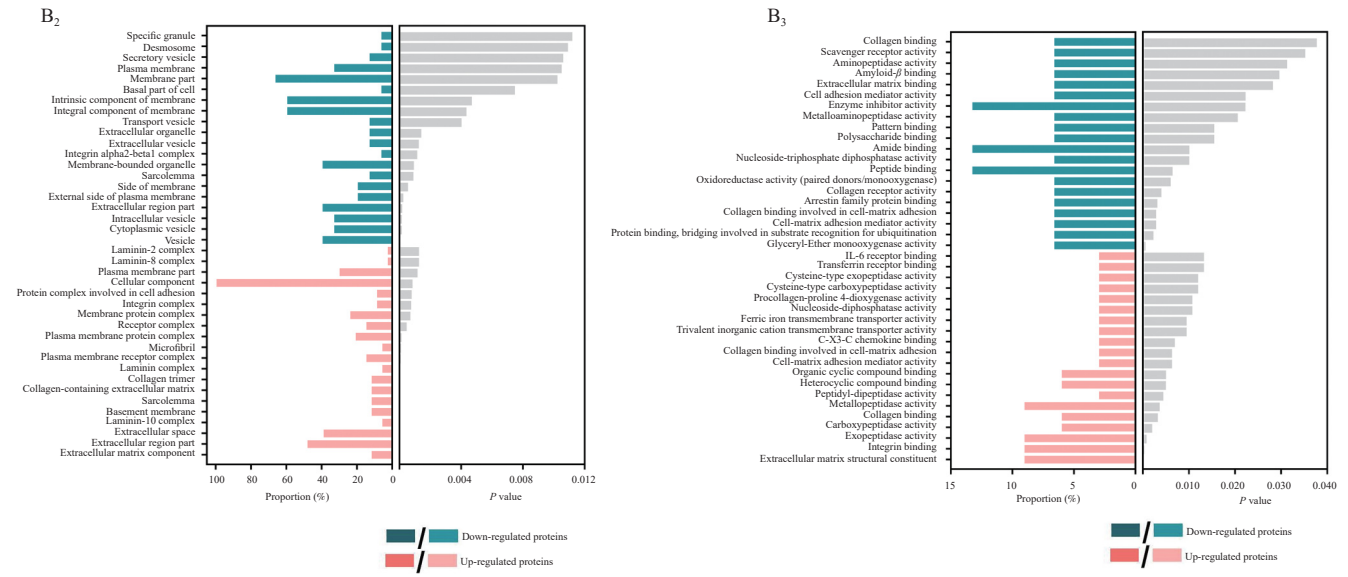

Fig. 7 (*Continued*)

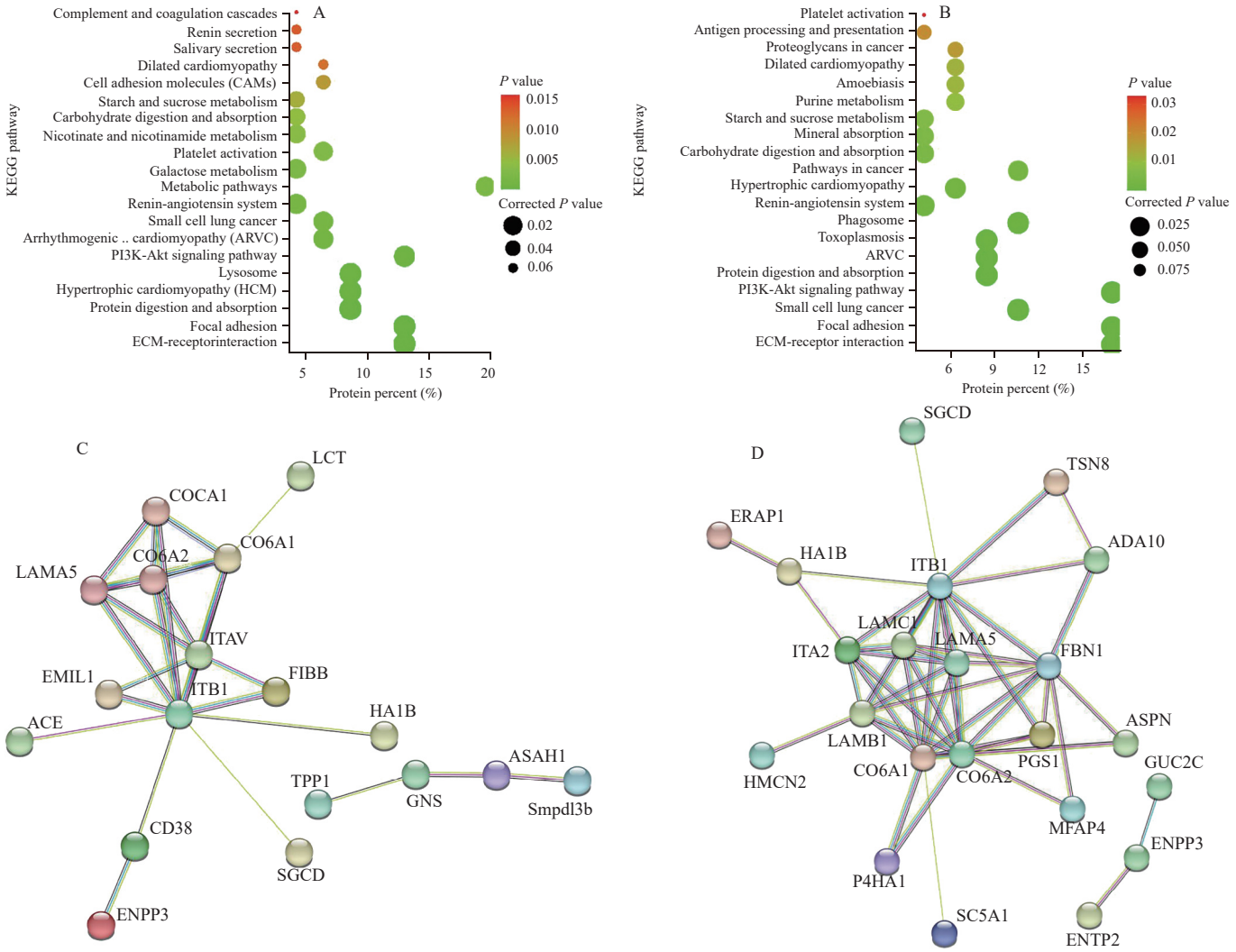

Fig. 8 KEGG enrichment analysis and STRING analysis of differentially expressed glycoproteins in the intestine of mice with tropomyosin allergy identified by precision *N*-glycoproteomics. KEGG enrichment analysisbased on (A) 6-samples and (B) 4-samples; STRING analysis based on (C) 6-samples and (D) 4-samples. ARVC, arrhythmogenic right ventricular cardiomyopathy.

(in the 4-sample analysis), and metabolic pathway (in the 6-sample analysis). Additionally, numerous disease-related pathways, including cancer pathways and the arrhythmogenic right ventricular cardiomyopathy pathway, among others, were enriched, suggesting a potential link between food allergy and cardiovascular system health, intestinal tumors, or inflammation.

Lastly, a quantitative protein-protein interaction (PPI) analysis using STRING showed that collagen (CO6A1/ CO6A2) exhibited the most interactions with other glycoproteins (Figs. 8C and D, Table S6). In addition to its receptor integrins (ITAV/ITB1/ITB2), collagen was found to interact with laminin (LAMA5), fibrillin1, and disaccharide (Biglycan), along with lactase (LCT), sodium-glucose cotransporter 1 (SLC5A1), asporin, and prolyl 4-hydroxylase alpha (P4HA1), involved in digestion, cell adhesion, tissue structure and stability, cell signal transduction, and more. These results underscore the significant role of the ECM in the pathogenesis of tropomyosin allergy.

4. Discussion

Shellfish, particularly shrimp, is a leading cause of food allergies worldwide. Currently, no effective treatment for shellfish allergies exists. In the present study, we aimed to identify a new therapeutic target for seafood allergy by investigating the mechanism of tropomyosin sensitization from a glycobiological perspective using high-throughput mass spectrometry combined with the pGlyco3.0 search engine.

First, we sensitized mice with tropomyosin, the primary allergenic protein in seafood. Allergy symptom scores, tropomyosin-specific IgE, IgG1, inflammatory mediator histamine, and Th2-type inflammatory factors IL-4 and IL-13 levels were significantly higher in tropomyosin-sensitized mice than in the control group, indicating a typical IgE-mediated Th2 immune response. Histology analysis, expression of intestinal tight junction protein, and serum DAO levels further demonstrated the damage to the intestinal barrier caused by tropomyosin sensitization in allergic mice. The severity of damage decreased successively from the duodenum, through the jejunum and ileum, to the colon, which was consistent with the results of Lam et al.[8].

Given the extent of damage observed, the jejunum was selected for a detailed study of intestinal protein glycosylation. Precision *N*-glycoproteomic analysis identified 2 283 glycosylation peptides corresponding to 655 unique glycosylation sites in 399 proteins. Differential expression analysis demonstrated changes in the intestinal glycome triggered by idiopathic inflammation from allergens. Furthermore, we linked food allergies to ECM remodeling *via* enrichment analysis of the altered glycoproteins.

Significant enrichment in the ECM-receptor interaction pathway and focal adhesion pathway through KEGG pathway analysis of differentially expressed glycoproteins. ECM remodeling is strongly associated with these 2 signal transduction pathways. Focal adhesion is a massive protein complex formed at the site where cells encounter the ECM, serving as an intra-tissue cell scaffold based on fibrin and glycosaminoglycan[33-34]. Intracellular signaling events are triggered when ECM binds to cells. Moreover, focal adhesion, as an ECM signal, is transmitted to the cell signal center, influencing cell survival, proliferation, and differentiation[35]. Previous studies have demonstrated that ECM remodeling plays a pivotal role in pathogenic signaling in intestinal inflammation[36]. On one hand, enzymes involved in ECM remodeling regulate intestinal inflammation. For example, IBD is linked to increased levels of collagenase-1 (MMP-1)[37], stromelysin-1 (MMP-3)[38], and gelatinase B[39-40]. Moreover, increased collagenase-3 (MMP-13) causes damage to the intestinal barrier, and its deficiency makes mice more susceptible to experimental colitis[41]. On the other hand, the ECM contributes to maintaining gut barrier integrity and homeostasis. In mice with a lumican (a type of ECM) deficit, an increase in colitis and tissue damage is seen[42]. Moreover, intestinal hyaluronic acid fragment deposition increases due to intestinal inflammation, inducing leukocyte infiltration and natural immunological activation[43-44]. Consequently, the enrichment of differentially expressed glycoproteins in the ECM-receptor interaction and focal adhesion pathways suggests a strong correlation between tropomyosin allergy and ECM remodeling.

In addition, the upregulated glycoproteins enriched in the ECM-receptor interaction and focal adhesion pathways primarily included collagen (CO6A1/2), laminin (LAMA5, LAMC1, and LAMB1), and integrin (ITAV and ITB1). Firstly, the damage to the gastrointestinal mucosa caused by tropomyosin sensitization might necessitate the synthesis of collagen and laminin as part of the wound healing response. Additionally, the up-regulated integrins, acting as receptors for collagen and laminin, may function as mechanosensitive molecules, sensing and transmitting extracellular changes and activating intracellular signaling pathways. Kang et al.[45] demonstrated that αVβ1 suppresses intestinal inflammation by serving as a receptor for semaphorin 7A produced by intestinal epithelial cells. However, excessive ECM deposition may also be associated with the disruption of the intestinal barrier, exacerbating food allergy reactions[45]. Furthermore, type 2 cytokines, such as IL-13, have been established as important regulators of ECM remodeling[46]. These cytokines can disrupt tight junctions between intestinal epithelial cells, stimulate mucus production[47-49], and influence collagen-degrading enzymes[50], macrophage collagen synthesis[51], and collagen absorption and breakdown[51], supporting their role in tissue repair and remodeling[52]. This evidence contributes to the emerging understanding that the ECM plays a prominent role in tropomyosin allergy. However, additional research is needed to determine whether increased ECM levels have an anti-inflammatory or pro-inflammatory effect, and the specific role Th2 cytokines in this context.

Other signaling pathways linked to ECM remodeling were also enriched based on the differential glycosylation enrichment analysis. PI3K-Akt signaling cascade activation by Akt protein kinase begins with cell adhesion mediated by the ECM and integrin receptors on the cell surface, and down-regulation of laminin 5 has been demonstrated to inhibit PI3K-AKT-mTOR signaling pathway[53]. Moreover, PI3K-Akt signaling pathway upregulation has been associated with food allergies[54]. In addition, the enrichment of upregulated proteins in metabolic pathways may also be linked to ECM remodeling. Georgiadou et al.[55] found that the metabolic sensor adenosine monophosphate-activated protein kinase regulates α5β1-integrin and fibrillar adhesion assembly by influencing tensin synthesis, revealing an important connection between energy metabolism and ECM assembly[56]. These findings further underscore the link between ECM remodeling and tropomyosin allergy.

In conclusion, our findings provide a detailed description of the allergic intestinal glycome in a tropomyosin-allergic mouse model, enhancing our understanding of the connections between food allergies and the intestinal barrier. Furthermore, we stressed the critical correlation between tropomyosin allergy and ECM remodeling. However, certain issues remain unresolved. Firstly, these

ECM were highly glycosylated, and proteins with different glycosylation types exhibited varying levels of up-regulation, potentially serving alternative functions or affecting downstream signals. Additionally, the role of terminal sialylation and fucosylation modification of the intestinal ECM in food allergies needs to be studied, as the sialylation of mucins, such as mucin 2[10], have been proven to play an important protective role in maintaining intestinal mucus barrier homeostasis. Moreover, an anti-gelatinase neutralizing antibody is beneficial in reducing the symptoms of IBD in mice[57]. Additionally, a phase I clinical trial for a humanized anti-gelatinase B antibody has commenced (Clinical Trials.gov number: NCT01831427). The vast and untapped wealth of information within the allergic intestinal glycome could offer novel therapeutic targets. Consequently, a potentially effective method to treat food allergies would involve targeting ECM remodeling in a specific and fine-tuned manner to prevent allergen invasion by repairing intestinal barriers and maintaining the dynamic balance of intestinal tissue. In addition, assessing the severity of food allergies through quantification of biomarkers such as blood lipopolysaccharide levels or the activation of hepatic inflammatory signaling pathways (which constitute the intestine-liver axis) may shed light on alterations in glycosylation patterns across varying degrees of allergic responses. Such investigations could further our comprehension of the regulatory role of glycosylation and the underlying mechanisms involved in food allergy pathogenesis. Lastly, given the differences in glycosylation between humans and mice, for instance, humans contain only Neu5Ac while mice have 2 types of sialic acid, Neu5Ac and Neu5Gc; future studies elucidating the functional consequences of shifting glycosylation patterns are required, especially in the human body. This will establish a solid foundation for the development of novel treatments for food allergies.

5. Conclusion

Tropomyosin allergy may lead to alterations in the intestinal glycome and ECM remodeling. Additionally, a promising strategy for treating food allergies could involve precisely targeting the changes in the intestinal glycome and ECM remodeling. This approach aims to prevent allergen invasion by repairing intestinal barriers and maintaining the dynamic balance of intestinal tissues.

Conflict of interest

The authors declare no conflicts of interest.

Acknowledgements

Graphic abstract was modified from Servier Medical Art (https://smart.servier.com/), licensed under a Creative Common Attribution 3.0 Generic License (https://creativecommons.org/licenses/by/3.0/). We would like to thank Editage (www.editage.cn) for English language editing. This research was funded by the Tianfu Emei Plan (a talent program of Sichuan Province, China), awarded to Huilian Che.

Institutional review board statement

The study was conducted in accordance with the Declaration of Helsinki, and approved by the Human Research Ethics Committee of China Agricultural University (CAU-HR2021015) for studies involving humans. The animal study protocol was approved by the China Agricultural University's Experimental Animal Ethics Committee (AW70101202-4-1) for studies involving animals.

Informed consent statement

Informed consent was obtained from all subjects involved in the study.

Data availability statement

The original contributions presented in the study are included in the article/supplementary material, further inquiries can be directed to the corresponding authors.

Appendix A. Supplementary information

Supplementary data associated with this article can be found, in the online version, at http://doi.org/10.26599/FSHW.2024.9250247.

References

[1] L. Fu, C. Wang, Y. Zhu, Y. Wang, Seafood allergy: occurrence, mechanisms and measures, Trends Food Sci. Technol. 88 (2019) 80-92. https://doi.org/10.1016/j.tifs.2019.03.025.

[2] S. Gelis, M. Rueda, A. Valero, et al., Shellfish allergy: unmet needs in diagnosis and treatment, J. Investig. Allergol. Clin. Immunol. 30(6) (2020) 409-420. https://doi.org/10.18176/jiaci.0565.

[3] C.Y.Y. Wai, N.Y.H. Leung, K.H. Chu, et al. Overcoming shellfish allergy: how far have we come? Int. J. Mol. Sci. 21(6) (2020) 2234. https://doi.org/10.3390/ijms21062234.

[4] T. Ruethers, A.C. Taki, E.B. Johnston, et al., Seafood allergy: a comprehensive review of fish and shellfish allergens, Mol. Immunol. 100 (2018) 28-57. https://doi.org/10.1016/j.molimm.2018.04.008.

[5] L. Xu, L. Sun, H. Lin, A. Ishfaq, Z. Li, Allergenicity of tropomyosin of shrimp (*Litopenaeus vannamei*) and clam (*Ruditapes philippinarum*) is higher than that of fish (*Larimichthys crocea*) *via in vitro* and *in vivo* assessment, Eur. Food Res. Technol. 246 (2020) 103-112. https://doi. org/10.1007/s00217-019-03402-0.

[6] G. Reese, R. Ayuso, S.B. Lehrer, Tropomyosin: an invertebrate pan-allergen, Arch. Int. Allergy Immunol. 119 (1999) 247-258. https://doi.org/10.1159/000024201.

[7] P.M. Matricardi, J. Kleine-Tebbe, H.J. Hoffmann, et al., EAACI Molecular Allergology User's Guide, Pediatr. Allergy Immunol. 27 (2016) 1-250. https://doi.org/10.1111/pai.12563.

[8] Y.F. Lam, K.K. Tong, K.M. Kwan, et al., Gastrointestinal immune response to the shrimp allergen tropomyosin: histological and immunological analysis in an animal model of shrimp tropomyosin hypersensitivity, Int. Arch. Allergy Immunol. 167 (2015) 29-40. https://doi.org/10.1159/000431228.

[9] A.M. Kemter, C.R. Nagler, Influences on allergic mechanisms through gut, lung and skin microbiome exposures, J. Clin. Invest. 129(4) (2019) 1483-1492. https://doi.org/10.1172/JCI124610.

[10] Y. Yao, G. Kim, S. Shafer, et al., Mucus sialylation determines intestinal host-commensal homeostasis, Cell. 185 (2022) 1172-1188. e28. https://doi.org/10.1016/j.cell.2022.02.013.

[11] M. Matsuzawa, T. Ando, S. Fukase, et al., The protective role of conjunctival goblet cell mucin sialylation, Nat. Commun. 14(1) (2023) 1417. https://doi.org/10.1038/s41467-023-37101-y.

[12] Y. Zhang, X. Yu, M. Ichikawa, et al., Autosomal recessive phosphoglucomutase 3 (PGM3) mutations link glycosylation defects to atopy, immune deficiency, autoimmunity, and neurocognitive impairment, J. Allergy Clin. Immunol. 133(5) (2014) 1400-1409. https://doi.org/10.1016/j.jaci.2014.02.013.

[13] A. Parrish, M. Boudaud, A. Kuehn, et al., Intestinal mucus barrier: a missing piece of the puzzle in food allergy, Trends Mol. Med. 28 (2022) 36-50. https://doi.org/10.1016/j.molmed.2021.10.004.

[14] Z. Chen, J. Luo, J. Li, et al., Foxo1 controls gut homeostasis and commensalism by regulating mucus secretion, J. Exp. Med. 218(9) (2021) e20210324. https://doi.org/10.1084/jem.20210324.

[15] Z. Zhang, Z. Li, H. Lin, Reducing the allergenicity of shrimp tropomyosin and allergy desensitization based on glycation modification, J. Agric. Food Chem. 69 (2021) 14742-14750. https://doi.org/10.1021/acs.jafc.1c03953.

[16] E. De Angelis, R. Pilolli, S.L. Bavaro, et al., Insight into the gastro-duodenal digestion resistance of soybean proteins and potential implications for residual immunogenicity, Food Funct. 8 (2017) 1599-1610. https://doi.org/10.1039/c6fo01788f.

[17] R. Valdelvira, G. Garcia-Medina, J.F. Crespo, et al., Novel alimentary pasta made of chickpeas has an important allergenic content that is altered by boiling in a different manner than chickpea seeds, Food Chem. 395 (2022) 133586. https://doi.org/10.1016/j.foodchem.2022.133586.

[18] X.M. Li, D. Serebrisky, S.Y. Lee, et al., A murine model of peanut anaphylaxis: T- and B-cell responses to a major peanut allergen mimic human responses, J. Allergy Clin. Immunol. 106 (2000) 150-158. https://doi.org/10.1067/mai.2000.107395.

[19] R. Sepulveda, J.L. Longbottom, J. Pepys, Enzyme linked immunosorbent assay (ELISA) for IgG and IgE antibodies to protein and polysaccharide antigens of *Aspergillus fumigatus*, Clin. Allergy 9(4) (1979) 359-371. https://doi.org/10.1111/j.1365-2222.1979.tb02494.x.

[20] L. Yao, Z. Fan, S. Han, et al., Apigenin attenuates the allergic reactions by competitively binding to ER with estradiol, Front. Pharmacol. 11 (2020) 1046. https://doi.org/10.3389/fphar.2020.01046.

[21] D.C. Rio, M. Ares, G.J. Hannon, et al., Purification of RNA using TRIzol (TRI Reagent), Cold Spring Harb. Protoc. 5(6) (2010) prot5439. https://doi.org/10.1101/pdb.prot5439.

[22] K.J. Livak, T.D. Schmittgen, Analysis of relative gene expression data using real-time quantitative PCR and the $2^{-\Delta\Delta CT}$ method, Methods 25 (2001) 402-408. https://doi.org/10.1006/meth.2001.1262.

[23] Z. Zhang, X. Zhang, W. Chen, et al., Conformation stability, *in vitro* digestibility and allergenicity of tropomyosin from shrimp (*Exopalaemon modestus*) as affected by high intensity ultrasound, Food Chem. 245 (2018) 997-1009. https://doi.org/10.1016/j.foodchem.2017.11.072.

[24] L. Fu, S. Fu, C. Wang, et al., Yogurt-sourced probiotic bacteria alleviate shrimp tropomyosin-induced allergic mucosal disorders, potentially through microbiota and metabolism modifications, Allergol. Int. 68(4) (2019) 506-514. https://doi.org/10.1016/j.alit.2019.05.013.

[25] T. Liu, S. Navarro, A.L. Lopata, Current advances of murine models for food allergy, Mol. Immunol. 70 (2016) 104-117. https://doi.org/10.1016/j.molimm.2015.11.011.

[26] S.M.T. Nguyen, C.P. Rupprecht, A. Haque, et al., Mechanisms governing anaphylaxis: inflammatory cells, mediators, endothelial gap junctions and beyond, Int. J. Mol. Sci. 22(15) (2021) 7785. https://doi.org/10.3390/ijms22157785.

[27] S. Anvari, J. Miller, C.Y. Yeh, et al., IgE-mediated food allergy, Clin. Rev. Allergy Immunol. 57 (2019) 244-260. https://doi.org/10.1007/s12016-018-8710-3.

[28] H. Yang, Y. Qu, Y. Gao, et al., Research progress on the correlation between the intestinal microbiota and food allergy, Foods 11 (2022) 2913. https://doi.org/10.3390/foods11182913.

[29] Y.Y. Cao, Y. Qiao, Z.H. Wang, et al., The polo-like kinase 1-mammalian target of rapamycin axis regulates autophagy to prevent intestinal barrier dysfunction during sepsis, Am. J. Pathol. 193 (2023) 296-312. https://doi.org/10.1016/j.ajpath.2022.11.008.

[30] M.Q. Liu, W.F. Zeng, P. Fang, et al., PGlyco 2.0 enables precision *N*-glycoproteomics with comprehensive quality control and one-step mass spectrometry for intact glycopeptide identification, Nat. Commun. 8 (2017) 438. https://doi.org/10.1038/s41467-017-00535-2.

[31] L. Wang, C. Huang, Z. Li, et al., Liquiritin inhibits MRGPRX2-mediated pseudo-allergy through the PI3K/AKT and PLCγ signaling pathways, Heliyon 9 (2023) e13290. https://doi.org/10.1016/j.heliyon.2023.e13290.

[32] F.L. Klaus, C. Kirsch, J.P. Müller, et al., PI3Kγ is a novel regulator of TNFα signaling in the human colon cell line HT29/B6, Ann. N. Y. Acad. Sci. 1515 (2022) 196-207. https://doi.org/10.1111/nyas.14842.

[33] D.A. Calderwood, Integrin activation, J. Cell Sci. 117 (2004) 657-666. https://doi.org/10.1242/jcs.01014.

[34] B.D. Stamper, S.S. Park, R.P. Beyer, et al., Differential expression of extracellular matrix-mediated pathways in single-suture craniosynostosis, PLoS One 6 (2011) e26557. https://doi.org/10.1371/journal.pone.0026557.

[35] Z.G. Gong, Y. Zhao, Z.Y. Wang, et al., Epigenetic regulator BRD4 is involved in cadmium-induced acute kidney injury *via* contributing to lysosomal dysfunction, autophagy blockade and oxidative stress, J. Hazard Mater. 423(Pt A) (2022) 127110. https://doi.org/10.1016/j.jhazmat.2021.127110.

[36] E. Shimshoni, D. Yablecovitch, L. Baram, et al., ECM remodelling in IBD: innocent bystander or partner in crime? The emerging role of extracellular molecular events in sustaining intestinal inflammation, Gut 64 (2015) 367-372. https://doi.org/10.1136/gutjnl-2014-308048.

[37] A. Wiercinska-Drapalo, J. Jaroszewicz, R. Flisiak, et al., Plasma matrix metalloproteinase-1 and tissue inhibitor of metalloproteinase-1 as biomarkers of ulcerative colitis activity, World J. Gastroenterol. 9 (2003) 2843-2845. https://doi.org/10.3748/wjg.v9.i12.2843.

[38] A. Kofla-Dlubacz, M. Matusiewicz, M. Krzystek-Korpacka, et al., Correlation of MMP-3 and MMP-9 with crohn's disease activity in children, Dig. Dis. Sci. 57 (2012) 706-712. https://doi.org/10.1007/s10620-011-1936-z.

[39] A. Annaházi, T. Molnár, K. Farkas, et al., Fecal MMP-9: a new noninvasive differential diagnostic and activity marker in ulcerative colitis, Inflamm. Bowel Dis. 19 (2013) 316-320. https://doi.org/10.1002/ibd.22996.

[40] M.A. Manfredi, D. Zurakowski, P.A. Rufo, et al., Increased incidence of urinary matrix metalloproteinases as predictors of disease in pediatric patients with inflammatory bowel disease, Inflamm. Bowel Dis. 14 (2008) 1091-1096. https://doi.org/10.1002/ibd.20419.

[41] R.E. Vandenbroucke, E. Dejonckheere, F. Van Hauwermeiren, et al., Matrix metalloproteinase 13 modulates intestinal epithelial barrier integrity in inflammatory diseases by activating TNF, EMBO Mol. Med. 5 (2013) 1000-1016. https://doi.org/10.1002/emmm.201202100.

[42] K. Lohr, H. Sardana, S. Lee, et al., Extracellular matrix protein lumican regulates inflammation in a mouse model of colitis, Inflamm. Bowel Dis. 18 (2012) 143-151. https://doi.org/10.1002/ibd.21713.

[43] C.A. de la Motte, Hyaluronan in intestinal homeostasis and inflammation: implications for fibrosis, Am. J. Physiol Gastrointest Liver Physiol. 301 (2011) G945-G949. https://doi.org/10.1152/ajpgi.00063.2011.

[44] J. Webber, S. Meran, R. Steadman, et al., Hyaluronan orchestrates transforming growth factor-β1-dependent maintenance of myofibroblast phenotype, J. Biol. Chem. 284(14) (2009) 9083-9092. https://doi.org/10.1074/jbc.M806989200.

[45] V. Garlatti, S. Lovisa, S. Danese, et al., The multiple faces of integrin-ECM interactions in inflammatory bowel disease, Int. J. Mol. Sci. 22 (2021) 10439. https://doi.org/10.3390/ijms221910439.

[46] T.E. Sutherland, D.P. Dyer, J.E. Allen, The extracellular matrix and the immune system: a mutually dependent relationship, Science 379(6633) (2023) eabp8964. https://doi.org/10.1126/science.abp8964.

[47] K.B. Madden, L. Whitman, C. Sullivan, et al., Role of stat6 and mast cells in IL-4- and IL-13-induced alterations in murine intestinal epithelial cell function, J Immunol. 169(8) (2002) 4417-4422. https://doi.org/10.4049/jimmunol.169.8.4417.

[48] P.J.M. Ceponis, F. Botelho, C.D. Richards, et al., Interleukins 4 and 13 increase intestinal epithelial permeability by a phosphatidylinositol 3-kinase pathway. Lack of evidence for STAT 6 involvement, J. Biol. Chem. 275 (2000) 29132-29137. https://doi.org/10.1074/jbc.M003516200.

[49] K. Dabbagh, K. Takeyama, H.M. Lee, et al., IL-4 induces mucin gene expression and goblet cell metaplasia *in vitro* and *in vivo*, J. Immunol. 162 (1999) 6233-6237. https://doi.org/10.4049/jimmunol.162.10.6233.

[50] K.M. Vannella, T.A. Wynn, Macrophages in tissue repair, regeneration, and fibrosis, Immunity 44(3) (2016) 450-462. https://doi.org/10.1016/j.immuni.2016.02.015.

[51] M. Schnoor, P. Cullen, J. Lorkowski, et al., Production of type VI collagen by human macrophages: a new dimension in macrophage functional heterogeneity, J. Immunol. 180 (2008) 5707-5719. https://doi.org/10.4049/jimmunol.180.8.5707.

[52] R.L. Gieseck, M.S. Wilson, T.A. Wynn, Type 2 immunity in tissue repair and fibrosis, Nat. Rev. Immunol. 18 (2018) 62-76. https://doi.org/10.1038/nri.2017.90.

[53] X. Zhang, Q. Li, W. Jiang, et al., LAMA5 promotes human umbilical vein endothelial cells migration, proliferation, and angiogenesis and is decreased in preeclampsia, J. Matern. Fetal Neonatal Med. 33(7) (2020) 1114-1124. https://doi.org/10.1080/14767058.2018.1514597.

[54] H. He, X. Ji, L. Cao, et al., Lycopene alleviates food allergy by modulating the PI3K/AKT pathway in peanut-sensitized BALB/c mice, Immunobiology 228 (2023) 152731. https://doi.org/10.1016/j.imbio.2023.152731.

[55] M. Georgiadou, J. Lilja, G. Jacquemet, et al., AMPK negatively regulates tensin-dependent integrin activity, J. Cell Bio. 216 (2017) 1107-1121. https://doi.org/10.1083/jcb.201609066.

[56] E. Dornier, J.C. Norman, Tensin links energy metabolism to extracellular matrix assembly, J. Cell Bio. 216 (2017) 867-869. https://doi.org/10.1083/jcb.201702025.

[57] N. Sela-Passwell, R. Kikkeri, O. Dym, et al., Antibodies targeting the catalytic zinc complex of activated matrix metalloproteinases show therapeutic potential, Nat. Med. 18 (2012) 143-147. https://doi.org/10.1038/nm.2582.